Available online at www.sciencedirect.com
SCIENCE DIRECT®
International Journal of Mass Spectrometry 230 (2003) 65–70
International Journal of Mass Spectrometry
www.elsevier.com/locate/ijms

Stability of ion motion in the quadrupole ion trap driven by rectangular waveform voltages

Won-Wook Lee [a,b], Soon-Ki Min [b], Cha-Hwan Oh [a,b,*], Pill-Soo Kim [b], Seok-Ho Song [c], Mo Yang [d], Kyuseok Song [e]

[a] *Quantum Photonic Science Research Center, Hanyang University, Seoul 133-791, South Korea*
[b] *Department of Physics, Hanyang University, Seoul 133-791, South Korea*
[c] *Microoptics NRL, Department of Physics, Hanyang University, Seoul 133-791, South Korea*
[d] *Samyang Chemical Co. Ltd., Seoul 137-073, South Korea*
[e] *Laboratory for Quantum Optics, Korea Atomic Energy Research Institute, Taejon 305-600, South Korea*

Received 14 April 2003; accepted 15 August 2003

Abstract

The stability of ion motion in the Paul trap driven by rectangular waveforms was investigated. The stability region was determined by solving the equation of motion for an ion with fourth order Runge–Kutta method. The variation of stability region with the duty cycle was analyzed. The results showed the ability of mass analysis by changing the duty cycle without changing rf voltage. Also, a simple method of mass selection using rectangular waveforms was suggested.

Keywords: Mass spectrometer; Rectangular waveforms; Duty cycle; Mass analysis; Mass isolation

1. Introduction

Since Paul and Steinwedel invented a quadrupole ion trap using sinusoidal waveforms, the so called Paul trap [1], the ion trap has been widely applied to mass spectrometry [2,3], ion cooling and spectroscopy [4–6], frequency standards [7,8], quantum computing [9,10] and so on. Ion trap mass spectrometer has developed through several stages to its current stage of relatively high performance and increasing popularity [2,3]. To apply it to the various objectives, various waveforms of rf voltage to be applied to the quadrupole ion trap have been suggested [11–16]. Specially, the rectangular waveforms have received much attention of many research groups [11–15]. The rectangular waveforms are easier to generate and need lower rf voltage than the sinusoidal waveforms. With these interests, many groups, such as Ryazan State Radio Technical University [13,14] and Shimadzu Research Laboratory [15], have researched on the ion trajectory in Paul trap using rectangular waveforms.

When the rectangular waveforms are applied to the ring electrode of Paul trap, the stability region of Paul trap is changed. Richards et al. applied the rectangular waveforms to mass filter for the first time [11]. They studied the change of stability region and obtained the mass spectrum. Sadat Kiai investigated the characteristics of stability region of Paul trap using actuall pulse-forms [16], and Sheretov et al. suggested the general solution of Hill equation, of which Mathieu equation is the special solution [14]. They studied the ion trajectory of Paul trap using arbitrary waveforms and reported the various characteristics of Paul trap using rectangular waveforms as an example.

Although the usage of rectangular waveforms has many advantages, such as lower power requirement than the sinusoidal waveforms and the convenience to generate, most of the researches were limited by the characteristics of ion trajectory and stability region. In this paper, we studied the change of stability region due to the change of duty cycle of rectangular waveforms, and we suggested a new mass-selection method by adjusting the duty cycle.

* Corresponding author. Tel.: +82-2-2290-0926; fax: +82-2-2297-3812.
E-mail address: choh@hanyang.ac.kr (C.-H. Oh).

1387-3806/$ – see front matter © 2003 Elsevier B.V. All rights reserved.
doi:10.1016/j.ijms.2003.08.008

2. Stability region for an ion trap driven by rectangular waveforms

In Paul trap, time-varying quadrupole fields are used to confine the ions. Specially, Paul and Steinwedel chose the sinusoidal waveforms to generate time-varying quadrupole fields. The electric potential and equation of motion for z-direction are expressed by $\Phi(t) = U + V\cos(\Omega t + \phi)$ and $d^2z/d\xi^2 + (a_z - 2q_z\cos(2\xi))z = 0$, respectively. U and V are the dc voltage and the rf voltage with angular frequency Ω and phase difference ϕ, respectively. When we use the rectangular waveforms, the $\Phi(t)$ is replaced with

$$\Phi(t) = U + S_\delta(t) \tag{1}$$

where $S_\delta(t)$ is the rectangular waveforms with duty cycle δ as shown in Fig. 1(a). From $d^2Q/dt^2 = -(e/m)\nabla\Phi$, the equation of motion for an ion is as follows:

$$\frac{d^2Q}{d\xi^2} + (a_z - 2q_zS_\delta(\xi))Q = 0 \tag{2}$$

where Q is the canonical variable, the canonical time variable ξ is defined by $\xi = \Omega t/2$ and the $S_\delta(t)$ is rectangular waveforms as a function of the canonical time variable ξ, as shown in Fig. 1(b). The trap parameters, a_z and q_z, and angular frequency, Ω, are the same to the Paul trap. The change of stability region with the duty cyclesδ is shown in Fig. 2.

Each stability region was obtained by solving the Eq. (2) with fourth order Runge–Kutta method. In Fig. 2(a), the black line indicates the stability region for the sinusoidal waveforms that were by Paul and Steinwedel. And the gray line expresses the stability region for the rectangular waveforms with duty cycle $\delta = 0.500$. The boundaries of the stability region at $a_z = 0$ are 0.908 and 0.712 for the sinusoidal waveforms and rectangular waveforms, respectively. When the mass selective instability scan method is adopted to analyze mass spectrum, the rectangular waveform with $\delta = 0.500$ needs lower rf voltage to eject the ion from Paul trap than that needed by the sinusoidal waveforms. Fig. 2(b)–(d) shows the stability regions at various duty cycles of rectangular waveforms. If $\delta < 0.5$, $\beta_r = 0$ and $\beta_z = 1$ boundaries intersect the q_z-axis as shown in Fig. 2(b). If $0.5 < \delta < 0.65$, the q_z-axis intersects with both the $\beta_z = 0$ and $\beta_r = 1$ boundaries, as shown in Fig. 2(c). And if $\delta > 0.65$, the q_z-axis intersects the $\beta_z = 0$ and $\beta_r = 1$ boundaries at the same time, as shown in Fig. 2(d). These features are similar to the fact that the stability region rotates counter-clockwise as δ increases. In the stability diagram, heavy ions are located at low q_z. Fig. 2 shows that heavy ions and light ions can be stable or unstable according to δ. That is, when the mass instability scan method is adopted, the mass scan can be accomplished by changing only the duty cycle, without changing the rf voltage.

Table 1
The critical point values consist of stability diagram for duty cycle

	q_z	δ	Cuf-off mass (m/z)
a	0	0.568	–
b	0.340	0.568	<237.4
c	1.099	0.681	Only 73.4
d	1.132	0.650	>71.3
e	0.633	0.438	Only 127.5
f	0.160	0.483	<504.4
g	0.000	0.483	–

The cut-off masses indicated the mass limits for trapping in Paul trap when the rf frequency, rf voltage, and inner radius of ring electrode of Paul trap were fixed at 1.1 MHz, 1 kV and 10 mm, respectively.

The **H**s ($\mathbf{H}_r$ and $\mathbf{H}_z$) and **L**s ($\mathbf{L}_r$ and $\mathbf{L}_z$) points are the intersecting points between the boundary of stability region and $q_z = 0$ in Fig. 2. When all points of **H** and **L** for various duty cycles are connected, a stability diagram is re-defined by the loci of the **H** and **L** points, as shown in Fig. 3. Thus, Fig. 3 expresses the stability diagram for duty cycle in no dc voltage ($a_z = 0$), and consists of many connecting lines between **H** and **L** points for various duty cycles. The exact values of **a** to **f** in Fig. 3 are shown in Table 1. The solid lines connecting **b**–**c** and **d**–**e** are the boundaries which determine the ion's stability for z-direction. The solid lines connecting **c**–**d** and **e**–**f** determine the ion's stability for r-direction. Also, the solid lines connecting **a**–**b** and **f**–**g** were horizontal lines, so that the two lines provide only one intersecting point between δ_c-line and the stability diagram.

When we draw δ_c-line, on which δ is constant, in the region of the 0.568(**b**)$< \delta <$ 0.681(**c**), δ_c-line intersects the stability diagram at two points, **H** and **L**. These points correspond to **H** and **L** in Fig. 2(c). In this case, the stabilities of heavy ions and light ions in the Paul trap applying rectangular waveforms can be unstable for z-direction

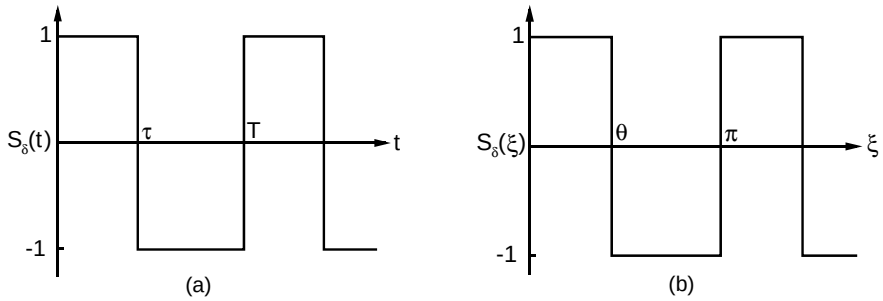

Fig. 1. Unit rectangular waveform (a) in terms of real time t, (b) in terms of the canonical time variable ξ. The duty cycle, δ, is defined by $\delta = \tau/T = \theta/\pi$.

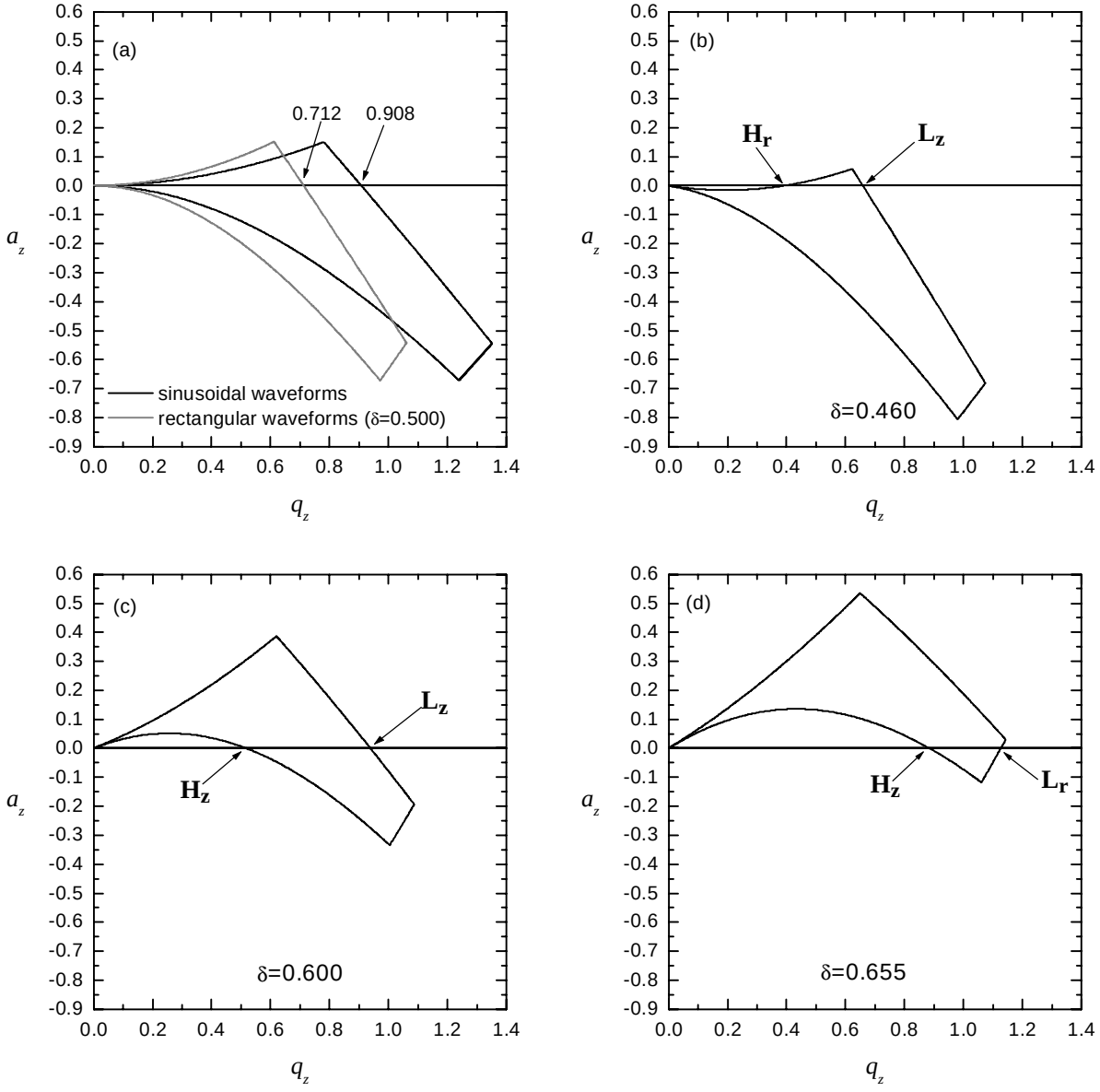

Fig. 2. The stability region. (a) The black line and gray line are the stability region for the sinusoidal waveforms and the rectangular waveforms of $\delta = 0.500$, respectively. (b), (c) and (d) are the stability regions using rectangular waveforms of $\delta = 0.460$, $\delta = 0.600$ and $\delta = 0.655$, respectively.

when q_z-value escapes the stability diagram in Fig. 3. However, the ion's stability is still stable for *r*-direction as in mass selective instability scan method. Also, δ_c-line intersects the stability diagram at just one point in the region of 0.483(**g**)$< \delta <$ 0.568(**a**), as shown in Fig. 2(a). When the q_z-value is increased incrementally at constant a_z, the trajectories of ions of low mass-to-charge ratio are rendered unstable first followed by those of ions of high mass-to-charge ratio. The regions of 0.438(**e**)$< \delta <$ 0.483(**f**) and 0.650(**d**)$< \delta <$ 0.681(**c**) correspond to the case of Fig. 2(b) and (d), respectively. When q_z-value in the regions escapes the stability diagram in Fig. 3, the ion's stability for *r*-direction or *z*-direction can be unstable according to the q_z-value. These regions are not useful since the ion's stability for *z*-direction is only used in practical mass spectrometry.

In other words, with increasing δ, δ_c-line moves up and heavy ions escape from the stability region, successively. With decreasing the δ, δ_c-line moves down and light ions also escape from the stability region, successively. Additionally, Fig. 3 can be divided into two regions, **A** and **B**. The **B** region has different features from that of the **A** region and is a specially interesting area. The many applications are possible using the **B** region shown in Fig. 4.

3. Mass analysis and mass selection

Fig. 4 shows only the **B** area in Fig. 3. The open circles from **b** to **e** were obtained by calculating Eq. (2). The solid δ_h-line is the fitted curve of open circles from **b** to **c**, and

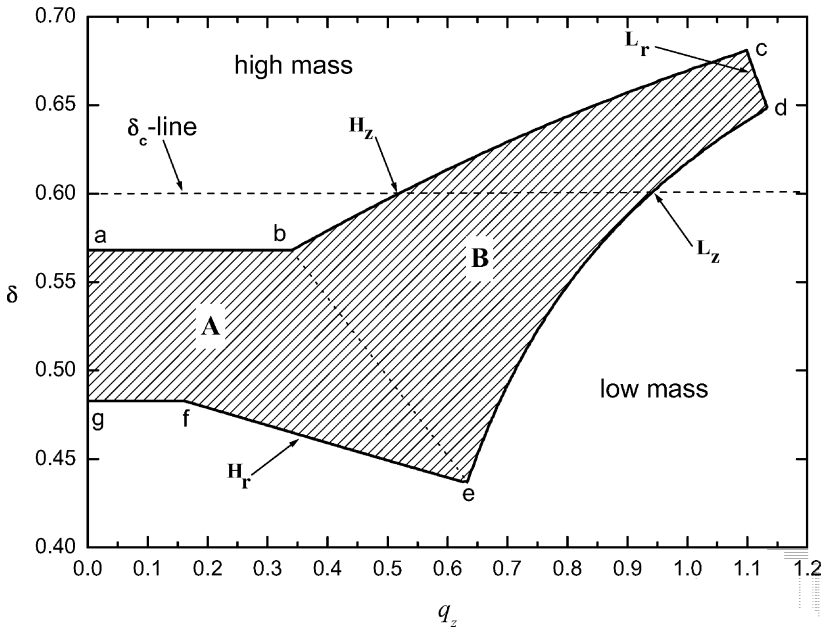

Fig. 3. The stability diagram for the various δs. The δ_c-line is the line which on δ is constant.

δ_l-line is the fitted curve of open circles from **d** to **e**. The equations of δ_h-line and δ_l-line are as follows:

$$\delta_h:\ \delta = 0.02099q_z^4 - 0.05699q_z^3 + 0.00166q_z^2 + 0.20314q_z + 0.5007 \quad (0.34 < q_z < 1.099) \tag{3}$$

$$\delta_l:\ \delta = -2.19719q_z^4 + 8.85769q_z^3 - 13.6706q_z^2 + 9.82661q_z - 2.1992 \quad (0.633 < q_z < 1.133) \tag{4}$$

Although Eqs. (3) and (4) have no physical meaning, Eqs. (3) and (4) give values of δ corresponding to q_z, which are useful to practically design a mass spectrometer. In Fig. 4, the dot lines indicated the q_z-value of 0.633, 0.712 and 0.908, respectively. The $q_z = 0.633$ is q_z-values of **e** point. The $q_z = 0.712$ is the maximum q_z of the stability region for $\delta = 0.500$ when $a_z = 0$. And the $q_z = 0.908$ is also the maximum q_z of the stability region for sinusoidal waveforms when $a_z = 0$. Using these dot lines, Fig. 4 is divided into four

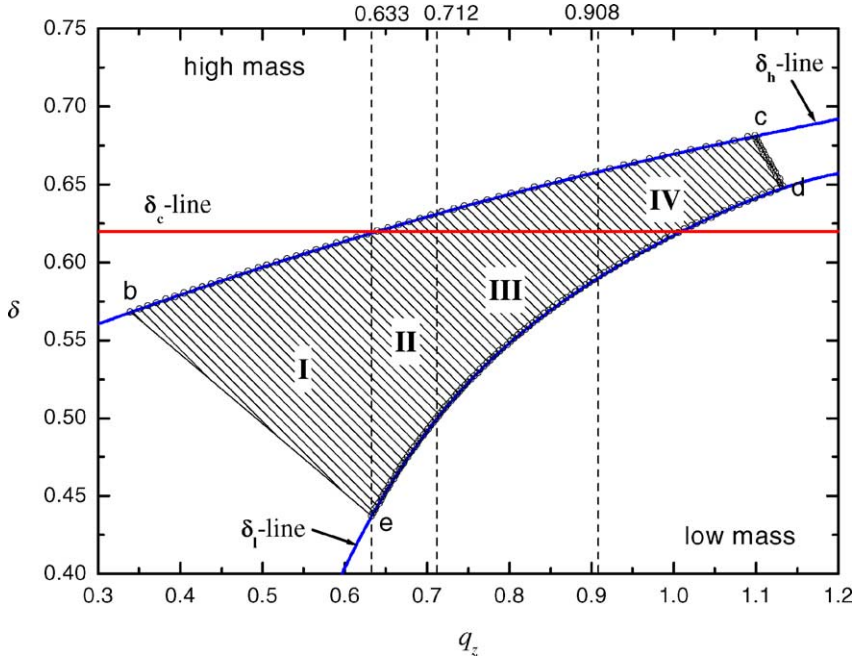

Fig. 4. The stability diagram enlarged **B** area in Fig. 3. δ_h-line and δ_l-line are the fitted curve of from **b** to **c** and from **d** to **e**.

regions. To apply to mass spectrometry, the IV-region is of little interest because we focused our interest on lower power consumption of mass spectrometer. The q_z-value is larger than that required 0.908 in this region. That is, higher rf voltage is needed than the case of the sinusoidal waveforms in this region. Therefore, the IV-region has a disadvantage to apply to the mass spectrometry, especially by the mass selective instability scan method, at lower rf voltage. When the III-region is used with mass selective instability scan method, there needs lower rf voltage is than needed in case of sinusoidal waveforms. However, this region needs higher rf voltage than rectangular waveforms for $\delta = 0.500$. Since the stability region of rectangular waveform with $\delta = 0.500$ is very similar to the stability region of sinusoidal waveforms as shown in Fig. 2(a), to use $q_z = 0.712$ of rectangular waveform at $a_z = 0$ is better than to use the III-region as for lower power consumption. The I- and II-regions have lower q_z than 0.712 and 0.908. Therefore, the lowest rf voltage needs to obtain the mass spectrum among the region mentioned above. However, when the I-region is used with mass selective instability scan method, ion's stability for *r*-direction is not guaranteed. Actually, the II-region is effective to apply to mass spectrometry at the lowest rf voltage. Additionally, the III- and IV-regions are also worth in a viewpoint of trap depth.

Applying Fig. 4 to mass selective instability scan method is simple. Draw the δ_c-line with $0.483 < \delta < 0.568$. The intersecting point between δ_c-line and δ_l-line play a role of $q_z = 0.908$ in the case of sinusoidal waveforms. For a given ion, ions are stable or unstable according to δ at fixed q_z. For example, when a rf voltage corresponding to $q_z = 0.650$ and $\delta = 0.575$ is applied to the ion trap, the δ_c-line can be drawn for $\delta = 0.620$. Then, ions with the masses from m_h to m_l can be trapped in the ion trap. Where m_h is maximum mass and is defined through intersecting q_z between δ_c-line and δ_h-line, and m_l is minimum mass and is defined as q_z between δ_c-line and δ_l-line. This feature is some different from the ordinary ion trapping technique. For the given rf voltage, all ions with some mass range are trapped in the ion trap. When the duty cycle increases, the heavy ions become unstable, and mass spectrum can be obtained. For example, the ions corresponding to intersecting q_z between δ_c-line and δ_h-line are unstable and ejected from ion trap, successively. The light ions are ejected from reversal process. This feature is very attractive. In general, the heavier the ion's mass is, the higher the rf voltage needed. However, in this method, only the change of duty cycle at fixed rf voltage gives the mass spectrum. Due to this advantage, not only the size of system can be small but also this feature is applied to the mass selection.

Fig. 4 can be transferred to Fig. 5 expressed by rf voltage instead of q_z. When it is assumed that there exist only three kinds of ion, and the mass of the ions is m_1, m_2 and m_3 ($m_1 < m_2 < m_3$), the regions that express the right diagonal lines, the left diagonal lines and the horizontal lines, are the stability diagrams for three kinds of ions (m_1, m_2 and m_3). With increasing mass of ions, the stability diagram moves to right. And there existed the overlapping area as can be seen in the figure. If the rf voltage with the duty cycle corresponding to *P* is applied to ion trap, all of the ions(m_1, m_2 and m_3) are trapped in the ion trap. Then, if the duty cycle is changed from *P* to *Q* suddenly, the ions of m_1 and m_2

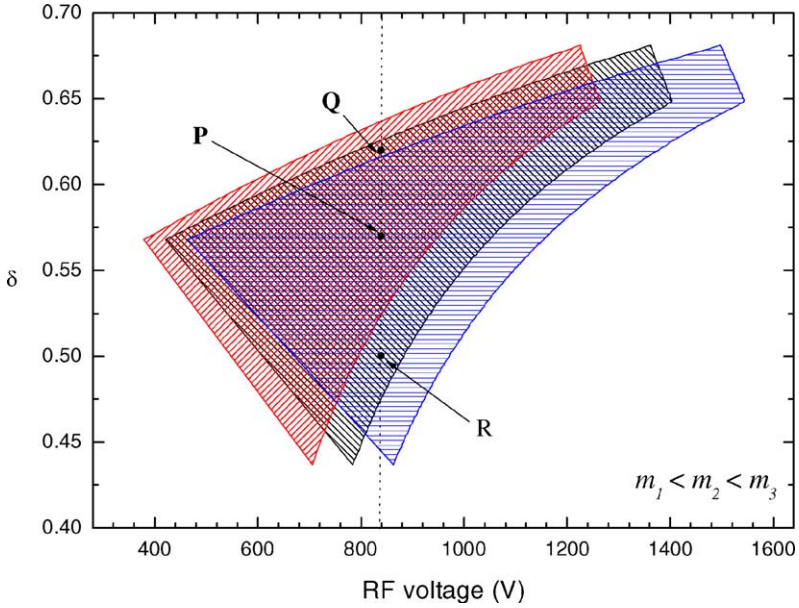

Fig. 5. The stability diagram for ions of various mass of ions. The right diagonal line, left diagonal line and horizontal line are the stability diagram for light ion, standard ion and heavy ion, respectively. The mass of each ion is m_1 (90 amu), m_2 (100 amu), and m_3 (110 amu). The geometry of Paul trap and angular frequency are fixed at $r_0 = 10$ mm and $\Omega = 2\pi \times 1.1$ MHz, respectively.

are still stable. But the ion of m_3 becomes unstable. Therefore, the heavy ion can be excluded. Next, the light ions can be excluded through change of duty cycle from Q to R. Mass selection is made through these processes. That is to say, ions are created (externally or internally) and stored in the ion trap driven by a rectangular waveform. Variation of the duty cycle can result in ejection of a selected range of ions of low mass-to-charge ratio and in ejection of a selected range of ions of high mass-to-charge ratio. One or more species may remain in the ion trap after the above variation of the duty cycle. Richards et al. suggested the similar method in mass filter [11], and Traldi and co-workers have discussed the method for the sinusoidal trap [2,17,18]. However, these processes need the fine tuning of duty cycle at high frequency. Actually, it is effective to use these processes and mass selective instability scan method at the same time.

4. Conclusion

When the rectangular waveform with arbitrary duty cycle was applied to the ion trap, the ion's stability region showed the various features. The stability region intersected only q_z-axis in $0.438 < \delta < 0.681$. The stability diagram as a function of duty cycle was re-defined. The stability diagram indicated that the ion's stability for only z-direction was changed in $0.483 < \delta < 0.650$ with the constant rf voltage. Also, when the rf voltage and duty cycle were fixed, the mass range of trapping ions in the Paul trap was determined in $0.568 < \delta < 0.650$. These characteristics of duty cycle suggested the simple methods of mass analysis and mass selection.

The suggested methods of mass analysis and mass selection have some advantages. The mass spectrometer using rectangular waveforms needs lower rf voltage than sinusoidal waveforms and is easy to generate. And these methods should simplify the system of mass spectrometer.

Acknowledgements

This research was supported by the Agency for Defense Development (project number: 01-DU-EB-01). Dr. C.-H. Oh wishes to acknowledge the financial support in part from the KOSEF through the Quantum Photonic Science Research Center at Hanyang University and the financial support of Hanyang University (HY-2002-S).

References

[1] W. Paul, H. Steinwedel, Z. Naturforsch. A 8 (1953) 448.
[2] R.E. March, F.J. Todd, Practical Aspects of Ion Trap Mass Spectrometry, CRC Press, New York, 1995.
[3] R. March, J. Mass Spectrom. 32 (1977) 263.
[4] D.J. Wineland, W.M. Itano, J.C. Bergquist, Opt. Lett. 12 (1987) 389.
[5] W.M. Itano, J.C. Bergquist, R.G. Hulet, D.J. Windeland, Phys. Rev. Lett. 59 (1987) 2732.
[6] W.M. Itano, D.J. Heinzen, J.J. Bollinger, D.J. Wineland, Phys. Rev. A 41 (1990) 2295.
[7] J. von Zanther, J. Abel, Th. Becker, M. Fries, E. Peik, H. Walther, R. Holzwarth, J. Reichert, Th. Udem, T.W. Hansch, A.Yu . Nevsky, M.N. Skvortsov, S.N. Bagayev, Opt. Commun. 166 (1999) 57.
[8] R.J. Rafac, B.C. Young, J.A. Beall, W.M. Itano, D.J. Wineland, J.C. Berquist, Phys. Rev. Lett. 85 (2000) 2462.
[9] D. Kielpinski, V. Meyer, M.A. Rowe, C.A. Sackett, W.M. Itano, C. Monroe, D.J. Wineland, Science 291 (2001) 1013.
[10] A. Steane, C.F. Roos, D. Stevens, A. Mundt, D. Leibfried, F. Schmidt-Kaler, R. Blatt, Phys. Rev. A 62 (2000) 042305.
[11] J.A. Richards, R.M. Huey, J. Hiller, Int. J. Mass Spectrom. Ion Phys. 12 (1973) 317.
[12] N.V. Konenkov, M. Sudakov, J. Am. Soc. Mass Spectrom. 13 (2002) 597.
[13] E.P. Sheretov, Int. J. Mass Spectrom. 219 (2002) 315.
[14] E.P. Sheretov, I.V. Philippov, T.B. Karnav, E.V. Fedosov, V.W. Ivanov, Int. J. Mass Spectrom. 219 (2002) 325.
[15] L. Ding, M. Sudakov, S. Kumashiro, Int. J. Mass Spectrom. 221 (2002) 117.
[16] S.M. Sadat Kiai, Int. J. Mass Spectrom. 188 (1999) 177.
[17] J. Gronowska, C. Paradisi, P. Traldi, U. Vettori, Rapid Commun. Mass Spectrom. 4 (1990) 306.
[18] C.E. Andanaz, P. Traldi, U. Vettori, J. Kavka, F. Guidugli, Rapid Commun. Mass Spectrom. 5 (1991) 5.